International Journal of Computer Information Systems and Industrial Management Applications.
ISSN 2150-7988 Volume 15 (2023) pp. 383-395

Classification of Parkinson's Disease in Brain MRI Images Using Deep Residual Convolutional Neural Network (DRCNN)

Puppala Praneeth[1], Majety Sathvika[2], Vivek Kommareddy[3], Madala Sarath[4], Saran Teja Mallela [5], Dr. K. Suvarna Vani[6] and Dr. Prasun Chkrabarti[7]

[1]Velagapudi Ramakrishna Siddhartha Engineering College, Kanuru, Vijayawada, Andhra Pradesh.
praneethpuppala6@gmail.com
[2]Velagapudi Ramakrishna Siddhartha Engineering College, Kanuru, Vijayawada, Andhra Pradesh.
majetysathvika9@gmail.com
[3]Velagapudi Ramakrishna Siddhartha Engineering College, Kanuru, Vijayawada, Andhra Pradesh.
kommareddyvivek481@gmail.com
[4]Velagapudi Ramakrishna Siddhartha Engineering College, Kanuru, Vijayawada, Andhra Pradesh.
madalasaraths@gmail.com
[5]Velagapudi Ramakrishna Siddhartha Engineering College, Kanuru, Vijayawada, Andhra Pradesh.
mallelasaran.245@gmail.com
[6]Velagapudi Ramakrishna Siddhartha Engineering College, Kanuru, Vijayawada, Andhra Pradesh.
vanikonerusuvarna@gmail.com
[7]ITM SLS Baroda University, Vadodara. *drprasunchkrabarti@gmail.com*

Abstract :**In our aging culture, neurodegenerative disorders like Parkinson's disease (PD) are among the most serious health issues. It is a neurological condition that has social and economic effects on individuals. It happens because the brain's dopamine-producing cells are unable to produce enough of the chemical to support the body's motor functions. The main symptoms of this illness are eyesight, excretion activity, speech, and mobility issues, followed by depression, anxiety, sleep issues, and panic attacks. The aim of this research is to develop a workable clinical decision-making framework that aids the physician in diagnosing patients with PD influence. In this research, we proposed a technique to classify Parkinson's disease by MRI brain images. Initially, normalize the input data using the min-max normalization method and then remove noise from input pictures utilizing a median filter. Then utilizing the Binary Dragonfly Algorithm to select the features. Furthermore, to segment the diseased part from MRI brain images using the technique Dense-UNet. Then, classify the disease as if it's Parkinson's disease or health control using the Deep Residual Convolutional Neural Network (DRCNN) technique along with Enhanced Whale Optimization Algorithm (EWOA) to get better classification accuracy. Here, we use the public Parkinson's Progression Marker Initiative (PPMI) dataset for Parkinson's MRI images. The accuracy, sensitivity, specificity, and precision metrics will be utilized with manually gathered data to assess the efficacy of the proposed methodology.**

Keywords: Deep Learning, Deep Residual Convolutional Neural Network, health control, Parkinson's disease, Dense-UNet, classification.

I. Introduction

In recent years, severe diseases have been detected and monitored using a lot of health informatics tools. The monitoring of Parkinson's disease (PD), is typically identified in persons over 60 using artificial learning-based information systems. Approximately 7 to 10 million individuals worldwide are affected by this illness, which is one of the most prevalent and rapidly expanding neurodegenerative conditions [1-3]. It is mostly caused by a shortage of dopamine (a neurotransmitter) in the human brain, and it manifests as both motor and non-motor symptoms, including dementia, voice/speech impairment, depression, sluggish thinking, stiffness, bradykinesia, and tremor [4]. A neurological condition known as Parkinson's disease is typically found in adults 50 years of age and older. Because the symptoms of Parkinson's disease are typically not captured or avoided until the patient is disturbed, the condition may initially go undetected. It is often characterized by neuronal degeneration in the human brain that results in the nervous system [5, 6]. Motor and Non-motor features are the two categories in which the original data obtained from the patients in the features form to classify PD is separated. A patient with Parkinson's disease may exhibit motor characteristics such as tremors, stiffness, and postural instability. While some instances of non-motor aspects are a patient's autonomic, cognitive, and sleep problems [7].

The condition of the patient's health is improved by an early diagnosis of PD, which also makes it easier for an experienced practitioner to make quick diagnoses. The traditional techniques used in the early recognition of PD rely exclusively on the information gathered from close examinations and patient interviews. These techniques don't use any kind of sophisticated computing on patient data. Some of the first non-intelligent methods used to diagnose PD were telemonitoring and telediagnosis systems [8-10]. Age is the main risk factor. Over 90 genes have been linked to a significant hereditary component of disease risk. Additionally, large populations have shown that some potentially modifiable environmental (such as water pollutants, and pesticides) and other factors (such as coffee, smoking, head trauma, or exercise) have a reason in the development of Parkinson's disease [11, 12].

Parkinson's disease begins with very modest and perhaps undetectable primary causes, but as the disease advances, the signs worsen. PD symptoms differ from person to person. PD begins with both non-motor and motor signs. Postural instability (loss of balance), Tremors, rigidity, and bradykinesia are examples of motor symptoms. Psychiatric symptoms, dysautonomia, motion sickness, and sensory impairment are examples of non-motor symptoms (autonomic dysfunction). Parkinson's patients frequently experience changes in speech, tremors, sluggish movement (bradykinesia), changes in handwriting, tight muscles, poor balance and posture, and loss of natural movements [13-15]. 90% of Parkinson's patients have vocal dysfunction issues, which is an early sign of the disease, according to research.

These vocal abnormalities include hypophonia (reduced volume), monotone (lower pitch), dysphonia (defective voice), and dysarthria (difficulties with articulation). It might be difficult to make an early detection of PD for a variety of reasons. Because most patients are over the age of sixty, it takes a lot of time for movement disorder specialists and neurologists to identify this disease after thoroughly analyzing the patient's full medical history and undergoing multiple scans [16]. When examining the patient's information and symptoms, the doctors' ability to correctly identify PD is based on their domain competence. But there are not enough skilled doctors' in developing countries like India, Brazil, Argentina, etc. So, recognizing or identifying PD is a difficult undertaking because professionals are stressed out by their heavy work. This makes us to develop a decision assistance system that would help medical professionals recognize PD.

In this paper, we proposed a technique to classify Parkinson's disease by MRI brain images. It has 4 steps to follow. Initially, normalize the input data using the min-max normalization method and then remove noise from input pictures utilizing a median filter. Then utilizing the Binary Dragonfly Algorithm to select the features. Furthermore, to segment the diseased part from MRI brain images using the technique Dense-UNet. Then, classify the disease as if it's Parkinson's disease or health control using the DRCNN technique along with Enhanced Whale Optimization Algorithm to get better classification accuracy. The key contributions of this paper are,

- In the pre-processing stage, we normalize the input data using the min-max normalization method and then remove the noise from the input image utilizing the median filter.
- To feature the selection process, utilizing the Binary Dragonfly Algorithm. Then using the Dense-UNet technique to segment the Parkinson's disease part in brain MRI images.
- We use the deep learning-based classification technique DRCNN to classify the disease if it's Parkinson's disease or normal health control along with Enhanced Whale Optimization Algorithm for better classification accuracy.

This article's remaining sections are organized as follows. Section 2 covers the relevant research on Parkinson's disease classification. Section 3 provides a thorough explanation of the proposed technique and its elements. Section 4 describes the experimental approach. Section 5 reviews the work and makes recommendations for further investigation.

II. Literature Review

In the literature survey, we reviewed some papers and mentioned all below. To detect Parkinson's disease, Solana et al. [17] recommended categorization of 3D MRI scans is created, applied to each gender, and the interpretation that follows. This is achievable since we employ the largest dataset that is currently accessible, where the amount of observations is sufficient for gender-specific dataset segmentation. Finding the most pertinent areas of interest for each gender is made possible by the usage of different sets for female and male subjects. (3) the use of multiple classifiers (Bayesian Network, Multi-Layer Perceptron, Naive Bayes, Random Forest, Support Vector Machine, k Nearest Neighbors, Logistic) for a binary decision. (1) The viability of second-order statistics for attribute retrieval. (2) The utilize of attribute chosen methods to find the most pertinent features while decreasing computational complexity. When the regions under study are additionally specified, the binary outcome from a classifier is of clinical use since doctors must comprehend the rationale for a recommendation by visually inspecting those regions on pictures.

Balaji et al. [18] presented a gait categorization method based on ML that can help the clinician identify the stages of PD. Gait pattern, which is important for evaluating human mobility, is a key biomarker for determining if a person has PD or is in good condition. Therefore, we use the VGRF gait dataset and use statistical analysis to determine the minimal feature vector. The Shapiro-Wilk test is then used to confirm that the data have a normal distribution, and the correlation-based feature chosen approach is then utilized to recognize the salient biomarkers from the temporal and spatial gait pattern features. For kinematic and statistical analyses that predict the severity of PD, four supervised machine learning algorithms Bayes classifier (BC), decision tree (DT), support vector machine (SVM), and ensemble classifier (EC) are utilized.

Sivaranjini & Sujatha [19] developed a technique to use deep learning architecture to categorize the MR pictures of PD and HC participants. The public domain database of PPMI is where the photographs needed for classification were found. The MR images are normalized as part of the pre-processing, and the normalized pictures are then subjected to a Gaussian filter. For classification, a convolution neural network known as the AlexNet model is used. To categorize the HC and PD participants, the pre-trained method's weights are utilized, and the final fully connected layer is refined using the right hyperparameters. The classification results are confirmed once the model has been trained to learn low-level to high-level features.

A DL model was created by Nagasubramanian and Sankayya [20] to identify Parkinson's disease. For generating a well-known data pattern, the methodologies utilized in this work are combined with HMM and absolute speech processing algorithms. To improve Parkinson's detection, a single heterogeneous dataset was created from numerous datasets. The approaches ARDNN, ADCNN, and ADNN are suggested for enabling multi-variant acoustic data processing activities based on these technological considerations. The suggested strategy used an appropriate data sampling approach to increase the accuracy rate. More disease-related occurrences were discovered due to the sampling. Results indicate that, in comparison to other existing works, the DMVDA functioned satisfactorily.

Speech problems are one of the earlier indicators of PD and can be utilized to make a detect. Caliskan et al. [21] suggested a Deep Neural Network (DNN) classifier for this purpose which includes stacked auto-encoders and softmax classifiers. To show the power of the deep neural network classifier, several simulations are run over two databases. The proposed classifier's findings are contrasted with those of the most recent classification methodology. The results of the experiment and the statistical analyses demonstrated how effective the deep neural network classifier is in diagnosing Parkinson's disease.

III. Proposed Methodology

PD is a central nervous system degenerative condition that primarily damages the motor activity in the brain cells. Parkinson's disease begins with very modest and perhaps undetectable primary causes, but as the disease advances, the symptoms worsen. PD symptoms differ from person to person. In this paper, we proposed a technique to classify Parkinson's disease by MRI brain images. It has 4 steps to follow. Initially, normalize the input data using the min-max normalization method and then remove noise from input pictures utilizing a median filter. Then utilizing the Binary Dragonfly Algorithm to select the features. Furthermore, to segment the diseased part from MRI brain images using the technique Dense-UNet. Then, classify the disease as if it's Parkinson's disease or health control using the DRCNN technique along with Enhanced Whale Optimization Algorithm to get better classification accuracy.

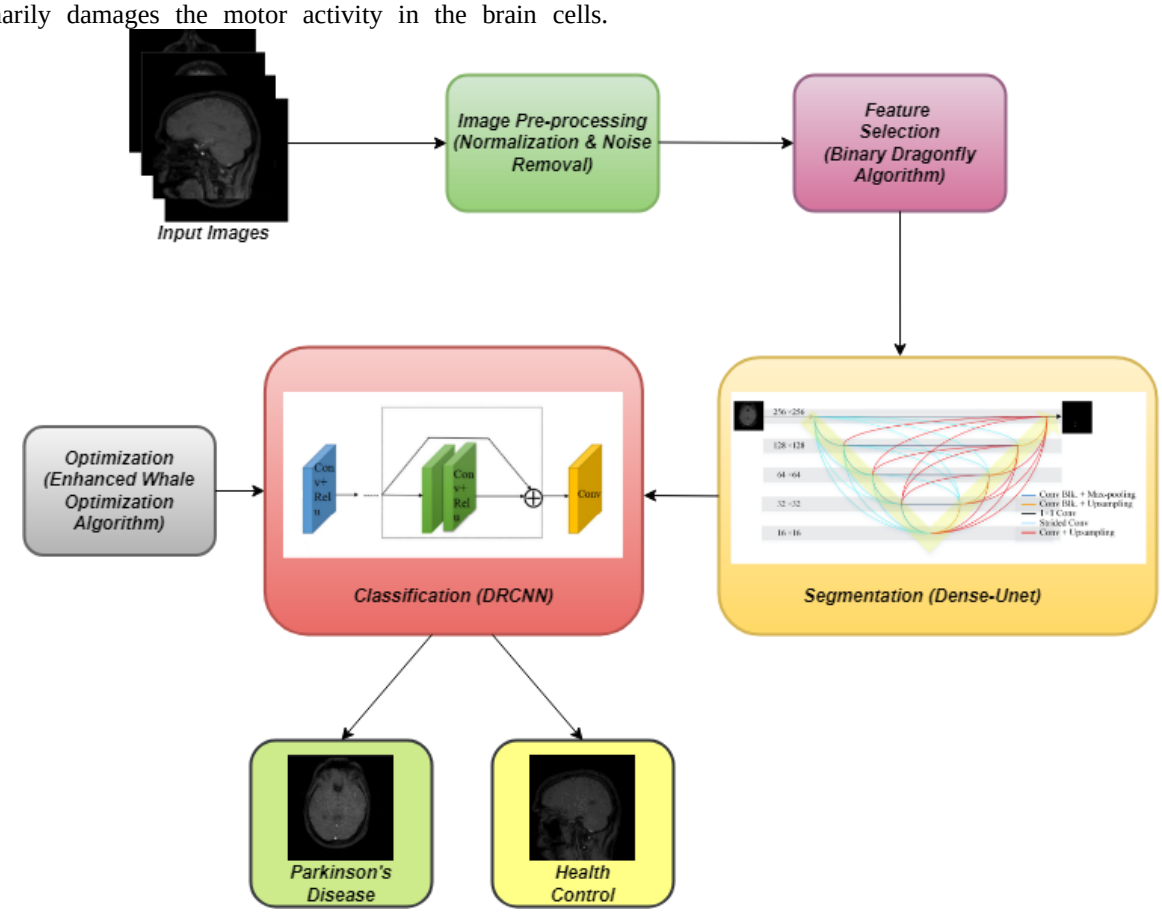

Figure 1. Structure of proposed methodology

The framework of the proposed techniques of PD classification is shown in Figure 1.

A. Image Preprocessing

Initially, in the preprocessing stage, we normalize the data and then remove noises from input images to better prediction of PD. To standardize the original data and speed up model convergence and increase model correctness, the Min-Max normalization method is chosen and is represented as

$$x = \frac{x - \min(x)}{\max(x) - \min(x)} \quad (1)$$

The method of normalization involves aligning and encapsulating MRI data to a thorough anatomic template. Because every person's brain differs in size and shape, normalization is necessary to make it easier to compare one brain MRI to another and translate the results into a standard shape and size. Normalization often involves mapping discrete subject-space data to a reference space with a template and a source image. The median filter, which employs a weighted average sum of the surrounding pixels, removes this noise. This filter does a great job of preserving the edges of an image. After data normalization, pictures are subjected to a median filter to remove noise.

B. Feature Selection

After preprocessing the input images, we need to select the features of brain MRI data. So here we use the Binary Dragonfly Algorithm (BDA) to feature selection. The Dragonfly Algorithm (DA), first described by [22] in 2016, has a discrete variant known as the Binary Dragonfly Algorithm. This algorithm imitates the natural swarming

behaviors of dragonflies. The interaction of dragonflies in avoiding the opponent (the worst solution) and locating the food source serves as a model for the exploitative and exploratory mechanisms of DA (the best solution). The position update mechanism in DA uses five primary behaviors: alignment, separation, attraction, cohesion, and distraction.

These actions are each explained as follows:

The goal of separation is to avoid a static collision between the current individual and a nearby individual. The following is how separation is expressed mathematically:

$$S_i = -\sum_{j=1}^{M} X - X_j \tag{2}$$

Where X is a dragonfly's location in a D-dimensional space (the D indicates the number of decision variables), X_j denotes the neighboring individual's location, and M denotes the number of neighbors.

Velocity matching between individuals in a sub-swarm or swarm is made possible through alignment. The calculation for alignment is as follows:

$$A_i = \frac{\sum_{j=1}^{M} V_j}{M} \tag{3}$$

Where M is the total amount of nearby individuals and V_j is their collective velocity.

The term "cohesion" describes the present individual's movement toward the middle of the group of nearby neighbors. The following definition of cohesion:

$$C_i = \frac{\sum_{j=1}^{M} X_j}{M} - X \tag{4}$$

Where M is the total amount of dragonflies in the area, and X_j is the dragonfly's position at the point j^{th}.

In natural swarms, people attract toward food sources and divert predators' attention in addition to alignment, cohesion, and separation. These two principle have also been mathematically modeled in the DA algorithm:

According to attraction, the person should be drawn to potential food sources. The attraction is defined mathematically as:

$$F_i = Xf - X \tag{5}$$

Where Xf denotes where a food source is located.

Distraction means that the person should be kept away from a predator by something external. The following is how the distraction is determined:

$$E_i = Xe + X \tag{6}$$

Where Xe denotes the enemy's location.

These five actions regulate how dragonflies migrate across DA. Each dragonfly's position is updated using the step vector generated as follows:

$$\Delta X_i(t+1) = (sS_i + \alpha A_i + cC_i + fF_i + eE_i) + w\Delta X_i(t+1) \tag{7}$$

Where s is the weight of separation, denotes alignment, c denotes cohesion weight, f denotes food weight, w denotes inertia weight, e denotes predator weight, and t denotes the current iteration.

The following equation is used to update the dragonfly positions in the original Digital Atlas:

$$X_i(t+1) = X_i(t) + \Delta X_i(t+1) \tag{8}$$

These movements and navigations enable this algorithm to address ongoing issues. In contrast to DA, BDA updates its position vectors using the following equations:

$$X_i^d(t+1) = \begin{cases} 1 - X_i^d(t) & rand < TF\left(\Delta X_i^d(t+1)\right) \\ X_i^d(t) & rand < TF\left(\Delta X_i^d(t+1)\right) \end{cases} \tag{9}$$

$$TF(\Delta X) = \left|\frac{\Delta X}{\sqrt{\Delta X^2+1}}\right| \tag{10}$$

where X_i^d is the location of the i^{th} dragonfly in the d^{th} iteration, *rand* displays a number produced at random between 0 and 1, t denotes the current iteration, ΔX is the step vector and $TF(.)$ is the transfer function as illustrated in Equation (9).

The BDA can frequently supply various global and local searches during the optimizations using separation, alignment, and cohesion. The other elements that enable the dragonflies to take advantage of the best options and avoid the bad ones are attraction and distraction. The BDA algorithm is superior due to these five swarming tendencies. The BDA approach is to select the features correctly.

C. Segmentation

After feature selection, we utilized the Dense-UNet technique to segment the abnormal part in MRI brain images. Resolution loss occurs as a result of the four down-samplings that U-Net typically does before the concatenate process. Because of the consequent resolution loss, extensional techniques are needed to increase accuracy. These techniques rely on deep network structures rather than shallow ones. For these reasons, we adopted the dense concatenated U-Net, termed Dense-UNet. The central point behind our proposed Dense-UNet is that it may be created by boosting the information flow across the model. For CXR images, convolution layers yield intermediate feature maps that are very similar to one another. To fully exploit the feature maps' capacity and avoid redundancies, a connection pattern is used, which greatly lowers computing costs. The input of the subsequent layers in Dense-UNet is created by concatenating the outputs of several intermediary layers.

The created feature maps from prior levels are used in all subsequent layers in the planned version of the U-Net, which uses dense connectivity (Fig. 2).

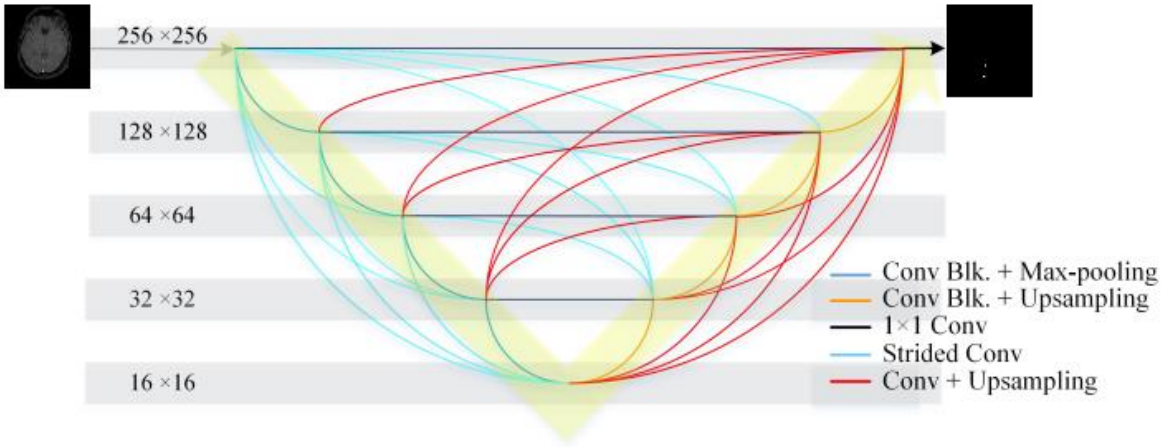

Figure 2. The proposed Dense-UNet model Architecture

The layers have immediate access to all prior maps during feedforward passes. This adds multi-level properties to the layer, which allows for the integration of various level maps. Additionally, learning is simpler in the backward gradient flow because of deep supervision; gradients can spread throughout all layers, even primary ones [23]. The loss function's profound impact on the model's many layers makes convergence easier, and information flow allows for a model with lighter construction and much fewer parameters that yet perform well.

The connections in Fig. 2 extract features and balance the size of transferred maps. Between the network's 9 tiers, there are $\frac{9\times(9-1)}{2} = 36$ connections between them. To solve the issue of uneven sizes within distinct layers, stride convolutions, max-pooling, and up-sampling techniques are applied. Equation (11) provides the dimensions of the output feature maps.

$$n_{out} = \left[\frac{n_{in}+2p-k}{s}\right] + 1 \qquad (11)$$

Where *p* displays the padding value around the map, *s* is the stride step, *k* is the kernel size, and n_{out} and n_{in} are the sizes of the output and input tensors, respectively. The architecture in Fig. 2 is described in depth as follows:

- Dark blue lines represent the procedures utilized in the Dense-main UNet's body, the max-pooling, and the convolution block (down-sampling by 2). Two convolution layers are the first two parts of a convolution block, which is then followed by a rectified linear activation function and batch normalization.
- The up-sampling and convolution blocks in the expansion path are represented by orange lines. These produce feature maps that are *2n* times as large as the input map.
- The 1x1 Conv connection (in black) simply modifies the depth of feature maps while extracting features; it does not alter the size of the maps. The final segmentation mask is created by transferring feature maps between the output layer and the matching layers.
- Stride convolution layers, represented by the light blue lines, produce smaller-scale feature maps. As seen in Fig 2, these connections transfer maps to the decoder from the encoder while tunings are used to modify the map sizes.
- The final connection type is represented by the red lines, which include an up-sampling process with scaling factors of 2, 4, and 8.

This Dense-UNet technique segment the diseased part in brain MRI images to better classification of the disease.

D. Classification

In the classification step, we employ the Deep Residual Convolution Neural Network technique to classify the disease after segmentation. This deep learning technique works effectively in MRI images. The nonlinear, dynamic, and correlative nature of the variables in complex industrial processes makes it important for latent feature representation to build a DRCNN (Deep Residual Convolutional Neural Network) method [24]. In contrast to shallow architectures, deep architectures created using the principle of deep learning may reflect complex characteristics and unidentified patterns from countless factors.

The DRCNN network model, which is designed to classify Parkinson's disease, is displayed in Fig 3. The network model is made up of a lot of blocks, a completely linked layer, and a pooling layer. A unit is a grouping of four connected blocks. Each filter in every unit is a 3x3 filter, which is the most effective. The number of filters in units 1, 2, and 3 are 16, 32, and 64, respectively, to provide multidimensional feature representation as the network becomes deeper. Every convolutional layer, except the first convolutional layer in units 2 and 3, uses stride equal to 1 and zero padding to ensure that output matrices are the same size as input matrices. In units 2 and 3, if the input matrices size is more than 4x4, the stride equals 2 in the first convolutional layer. To integrate the features and provide a little shift invariance, the matrices are reduced by half. The 64 matrices are combined by the average pool layer into a 64-tuples vector, which serves as the network's final feature representation. The 64-tuples vector is changed by the fully connected layer into a vector with the same number of tuples as faults. This vector is used to

calculate the loss function. The backpropagation algorithm may determine the gradients of the network using the loss function. The momentum update technique is used to update the network's properties.

Since the DRCNN model is a peer-to-peer deep learning network method, it can make predictions based on the input data directly. The DRCNN classification model is initially developed using a training set. After a significant number of iterations, the DRCNN method can comprehend the complex meaning of the input data and forecast the presence of failure. After entering the data,

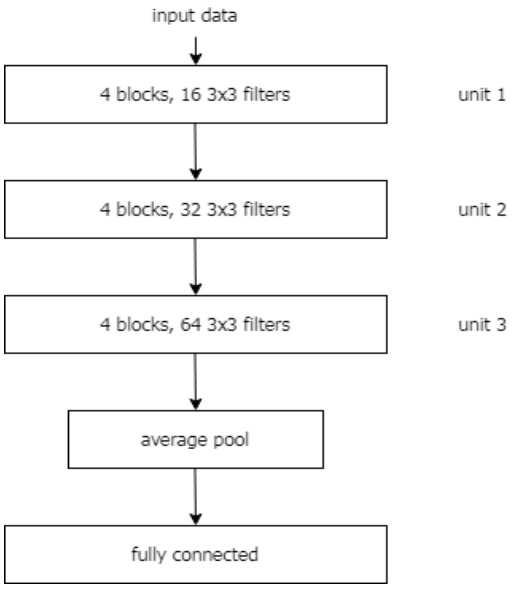

Figure 3. Classification using the DRCNN model.

This Deep Residual Convolutional Neural Network provides good classification results and accuracy. But we need to improve our proposed methodology performance, so proposed an optimization technique to get better classification accuracy.

E. Optimization Algorithm

To classify Parkinson's disease with effective accuracy, here we proposed an optimization algorithm's Enhanced Whale Optimization Algorithm (EWOA). The WOA was recently added to metaheuristic algorithms by [25]. The WOA is modeled after the bubble-net hunting approach used to kill humpback whales. They favor hunting small fish or krill schools that are near the surface. To make characteristic bubbles along a circle or "9"-shaped path, humpback whales swim around the prey in a shrinking circle and along a spiral-shaped path at the same time. There is a 50% chance of selecting either the encircling mechanism or the spiral model to update the position of whales during optimization to imitate this behavior in WOA. Their formulas are created in the following way:

1. *Encircling prey that is getting smaller:* In WOA, the best solution at the moment is presumed to be the target prey, and the other search agents attempt to adjust their locations in its direction. The following formula represents this behavior:

$$\vec{X}(t+1) = \vec{X}^*(t) - A.\vec{D} \quad (12)$$

$$\vec{D} = \left|C.\vec{X}^*(t) - \vec{X}(t)\right| \quad (13)$$

$$A = 2.a.r - a \quad (14)$$

$$C = 2.r \quad (15)$$

Where an is progressively decreasing from *2* to *0* for iterations, $\vec{X}$ is a whale location, $\vec{X}^*$ is the historically best position, *t* denotes the current iteration, and r is a random number with uniform distribution in the range [0, 1]. The absolute value is indicated by the notation "||".

2. *Spiral bubble-net feeding technique:* To replicate the helix-shaped movement of humpback whales, the following spiral equation is employed between the position of the whale and its prey:

3.

$$\vec{X}(t+1) = e^{bk}.\cos(2\pi k).\vec{D}' + \vec{X}^*(t) \quad (16)$$

$$\vec{D}' = \left|\vec{X}^*(t) - \vec{X}(t)\right| \quad (17)$$

Where *k* is a random number evenly distributed in the range [-1, 1] and *b* is a constant used to define the logarithmic spiral's shape.

When *A*<-1 or *A*>1, the search agent is updated by a random search agent rather than the best search agent to have a global optimizer:

$$\vec{X}(t+1) = \vec{X}_{rand} - A.\vec{D}' \quad (18)$$

$$\vec{D}'' = \left|C.\vec{X}_{rand} - \vec{X}(t)\right| \quad (19)$$

Where $\vec{X}_{rand}$ is chosen at random from the whales in the current iteration.

1) Enhanced Whale Optimization Algorithm (EWOA)

The WOA is effective in exploring global solutions because its basic premise is clear. A new algorithm known as the EWOA is presented to increase the search reliability, convergence speed, and solution accuracy of WOA. Maintaining the original method's simplicity is important while optimizing an algorithm.

Each iteration extracts a random number between [0, 1] for each whale. Equation (16) is picked if it is more than 0.5; else, Equation (21) is selected to update the position of the whale. In the EWOA exploration phase, one element of every whale is altered with a random value in the search space with a probability like *p* rather than Equation (18).

$$p = 0.3(1 - iter/iter_{max}) \quad (20)$$

Where $iter_{max}$ and $iter$, respectively, represent the total amount of iterations and the current iteration number for the optimization process.

An integer random number between [1, *ng*] is retrieved for each selected whale to determine which structure variable should be randomly altered. Next, the interval [0, 1] is used to extract another random amount, *q* which is then compared to the probability threshold *p*. According to $x_j = x_{jmin} + random.(x_{jmax} - x_{jmin})$, where a random amount evenly distributed in the range [0, 1], the chosen variable x_j is altered if *q*<*p*. The improved algorithm ought to be able to maintain a healthy balance between the tendencies toward intensification and diversification. This point and the change mentioned before indicate the definition of Equation (12) as follows:

$$\vec{X}(t+1) = \vec{X}^*(t) - \vec{A}\circ\vec{D}''' \quad (21)$$

$$\vec{D}' = \vec{r}\circ\left|\vec{X}(t)\right| \quad (22)$$

$$\vec{A} = 2.\vec{a}°\vec{r} - \vec{a} \quad (23)$$

Where $\vec{a}$ is a vector with every aspect equal to a and $\vec{r}$ is a random vector with every aspect equally distributed across the [0, 1] range. The symbol "°" designates a multiplication of elements one by one. The EWOA algorithm gives better accuracy for Parkinson's disease classification performance.

IV. Results And Discussion

The following part categorizes the PD utilizing the dataset's analysis and compares the method to "state-of-the-art" approaches. In the following subsections, provide the assessment results based on experimental information to evaluate technique.

A. Dataset Description

We employed the Parkinson's Progression Marker Initiative (PPMI) dataset's diffusion-weighted and T1 pictures. In this dataset, 412 individuals with a recent diagnosis of PD and 179 individuals in good health serve as controls. The medium age of PD patients is 61, while that of healthy people is 59. Over 93% of the participants are Caucasian, 71% of individuals with PD are men, and 57% of people with health conditions are men. PPMI dMRI data were collected from 32 different international sites utilizing a consistent technique for Siemens Tim Trio and Siemens Verio 3 Tesla MRI equipment. Utilizing a single b=0 picture and a b-value of 1000 s/mm2, 64 evenly distributed directions were covered by diffusion-weighted images. With a 2 mm isotropic resolution, 116x116 matrix, twofold acceleration, and TR/TE 900/88 ms, a single-shot echo-planar imaging (EPI) sequence was performed. Additionally, a 1 mm3 anatomical T1-weighted MPRAGE picture was captured. Two baseline acquisitions and two additional were performed on each patient a year later. The distribution of patients with right and left onsets is 57% and 43%, respectively. Visit http://www.ppmi-info.org for further details on MRI data collection and processing.

B. Quantitative Metrics

The evaluation performance of the proposed technique for categorizing the MRI brain images into PD or Health Control is to achieve a higher outcome. Here, are provided an input brain MRI picture from Parkinson's Progression Marker Initiative (PPMI) dataset. PD is a central nervous model degenerative condition that primarily damages motor activity in the brain cells. Parkinson's disease begins with very modest and perhaps undetectable primary causes, but as the disease advances, the symptoms worsen. This paper proposed a technique to classify Parkinson's disease from MRI brain images. Initially, normalize the input data using the min-max normalization method and then remove noise from input pictures utilizing a median filter. Then utilizing the Binary Dragonfly Algorithm to select the features. Furthermore, to segment the diseased part from MRI brain images using the technique Dense-UNet. Then, classify the disease as if it's Parkinson's disease or health control using the DRCNN technique along with Enhanced Whale Optimization Algorithm to get better classification accuracy. The outcomes of the evaluation performance are shown in Figure 4 below.

Original Picture	**After Noise Removal Picture**	**Segmented Pictures**	**Categorization of PD**
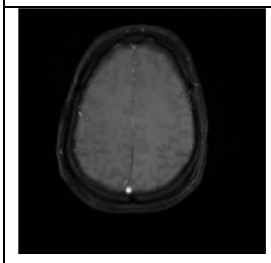	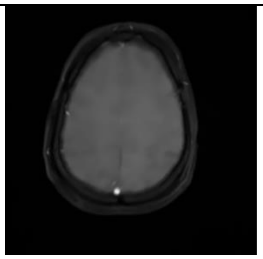		Parkinson's Disease Affected
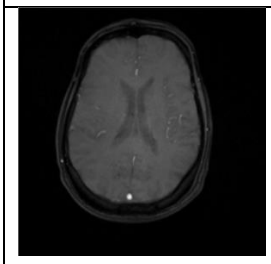	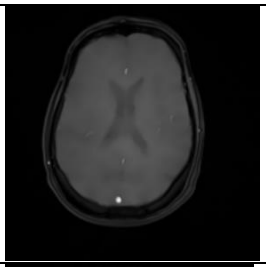	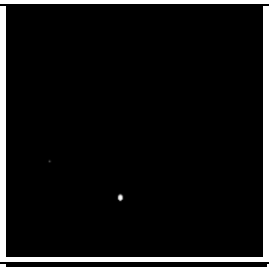	Parkinson's Disease Affected
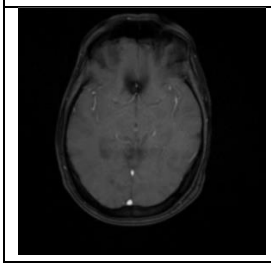	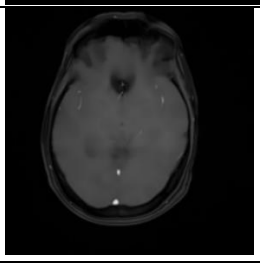	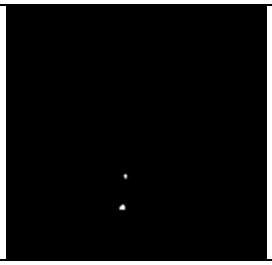	Normal Health Control

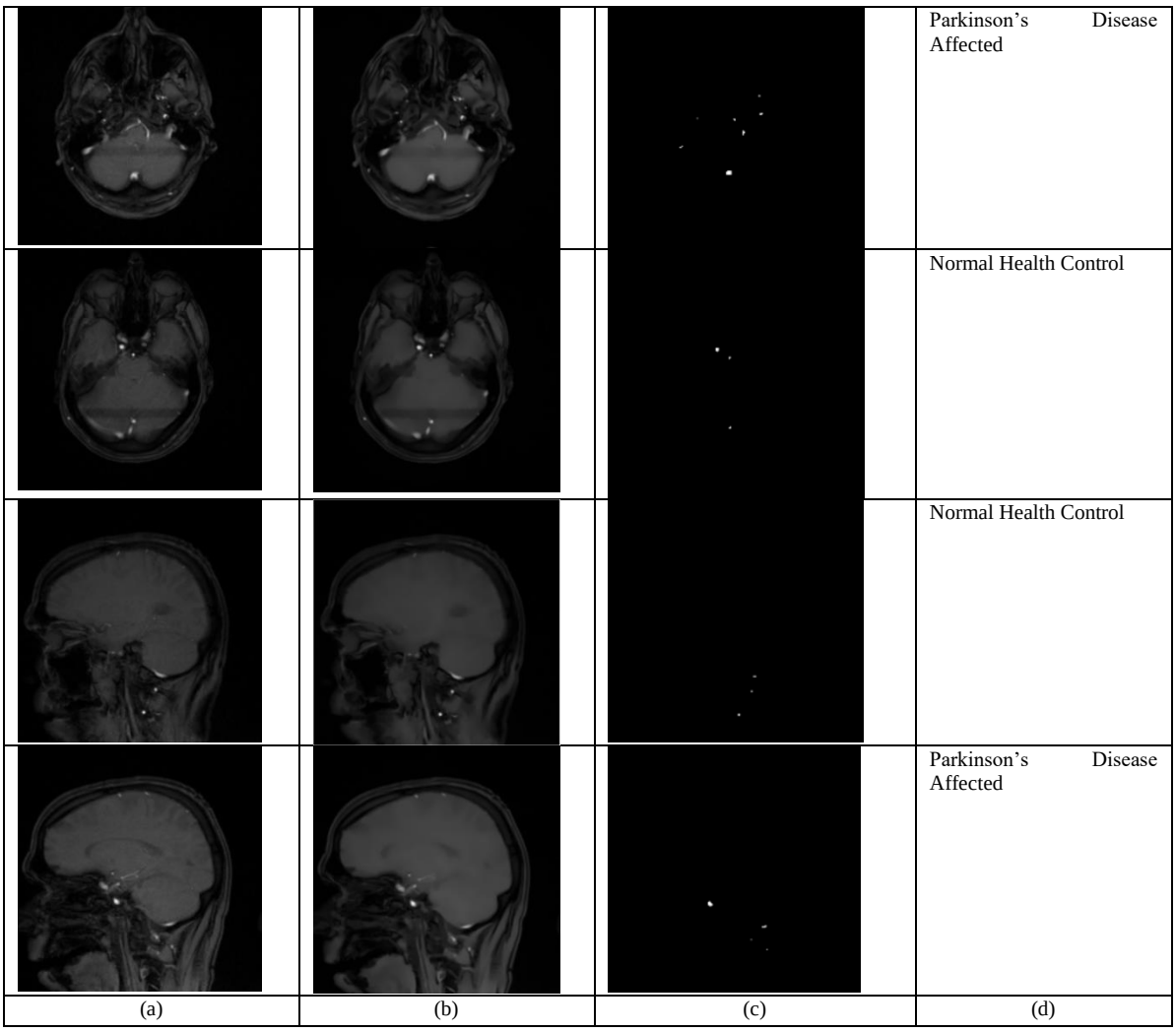

Figure 4. The performance evaluation outcomes: a) Original Picture, b) After Noise Removal Picture, c) Segmented Pictures, and d) Categorization of PD.

C. Evaluation Metrics

In regard to metrics for performance, consider the Accuracy, Sensitivity, Specificity, and Precision of the proposed method. These metrics indicate:

1) Accuracy

Accuracy is defined as the proportion of samples that were properly identified among all samples. A classifier generally performed higher its accuracy. Equation (24) illustrates the meaning of accuracy.

$$Accuracy = \frac{TP+TN}{TP+FN+FP+TN} \quad (24)$$

2) Sensitivity

Sensitivity, commonly referred to as recall, evaluates a classifier's ability to recognize positive samples by displaying the proportion of all projected positive samples. Equation (25) defines sensitivity.

$$Sensitivity = \frac{TP}{TP+FN} \quad (25)$$

3) Specificity

Specificity, which is expressed as the percentage of all incorrectly categorized negative samples, evaluates the classifier's ability to recognize negative samples. Equation (26) illustrates the definition of specificity.

$$Specificity = \frac{TN}{TN+FP} \quad (26)$$

4) Precision

The proportion of accurately predicted positive outcomes to all predicted positive observations is known as precision. The ability to carry out the following actions is precision.

$$Precision = \frac{TP}{TP+FP} \quad (27)$$

D. Performance Evaluation

Comparing proposed with the previous methods in experimental effectiveness, proposed has the best accuracy in classification. Table 1 demonstrates the outcomes for AlexNet [19], DMVDA [20], DNN [21], SVM [18], and the proposed DRCNN on the Parkinson's Progression Marker Initiative (PPMI) dataset in terms of specificity, accuracy, precision, and sensitivity. The proposed approach has greater accuracy for classification values than other previous methods, according to the results. So, we showed with optimization

algorithm and without optimization comparison results represented as a graph. The proposed method performed better in our database, according to the outcomes. Table 1 demonstrates our outcomes based on precision, specificity, accuracy, and sensitivity without optimization. Fig 5 displayed the accuracy analysis of the proposed technique without optimization accuracy compared with other previous approaches. And also Figure 6 demonstrated the comparison of the proposed approach's categorization outcomes with the previous approaches without optimization algorithm graphs for specificity, precision, and sensitivity. Our proposed model improved the classification accuracy with less computation time.

.

Approaches	Accuracy (%)	Sensitivity (%)	Specificity (%)	Precision (%)
AlexNet [19]	88.9	90.2	87.84	92.93
DMVDA [20]	93	93.81	89.10	90.76
DNN [21]	87.95	86.21	91.83	89.6
SVM [18]	95.4	92.64	93.12	94.73
Proposed (DRCNN)	97.22	95.93	94.45	96.98

Table 1 Using the proposed and compared approaches, calculate Precision, Specificity, Accuracy, and Sensitivity (%) without optimization

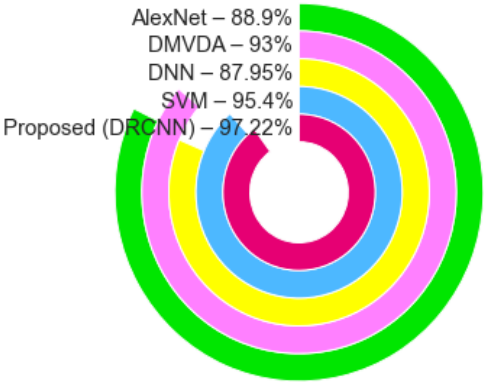

Figure 5. Analysis of Accuracy based on different techniques.

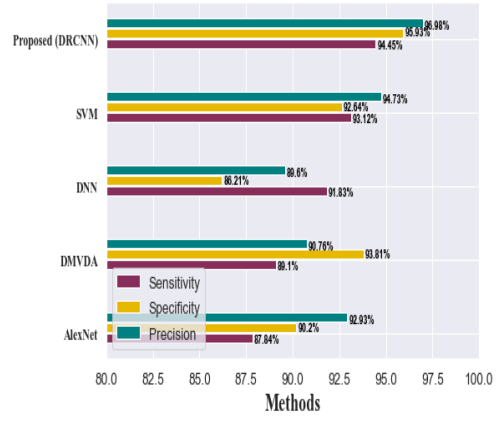

Figure 6. The proposed approach's categorization outcomes compared with existing approaches without optimization algorithm (a) Sensitivity, (b) Precision, and (c) Specificity.

Table 2 demonstrates our outcomes based on specificity, accuracy, precision, and sensitivity with an optimization algorithm. Fig 7 displayed the accuracy analysis of the proposed technique with optimization accuracy compared with the previous approaches. And also Figure 8 demonstrates the proposed approach's categorization outcomes compared with the previous approaches with optimization algorithm graphs for specificity, precision, and sensitivity. Table 2 demonstrates the outcomes for AlexNet [19], DMVDA [20], DNN [21], SVM [18], and the proposed DRCNN with EWOA technique on the PPMI dataset in terms of sensitivity, accuracy, precision, and specificity. Based on the outcomes, we can see that the proposed approach has higher categorization accuracy outcome value than other previous deep learning methods in terms of recognition rate sensitivity, accuracy, specificity, and precision.

Approaches	Accuracy (%)	Sensitivity (%)	Specificity (%)	Precision (%)
AlexNet [19]	88.9	90.2	87.84	92.93
DMVDA [20]	93	93.81	89.10	90.76
DNN [21]	87.95	86.21	91.83	89.6
SVM [18]	97.4	92.64	96.12	94.73
Proposed + Optimized (DRCNN)	98.87	96.87	98.13	97.02

Table 2 utilizing the proposed and compared methods, measures Precision, Specificity, Accuracy, and Sensitivity (%) optimization.

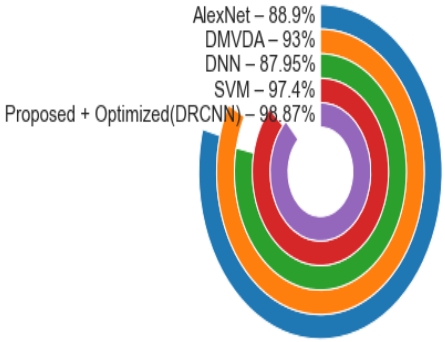

Figure 7. Comparison of Accuracy based on different approaches.

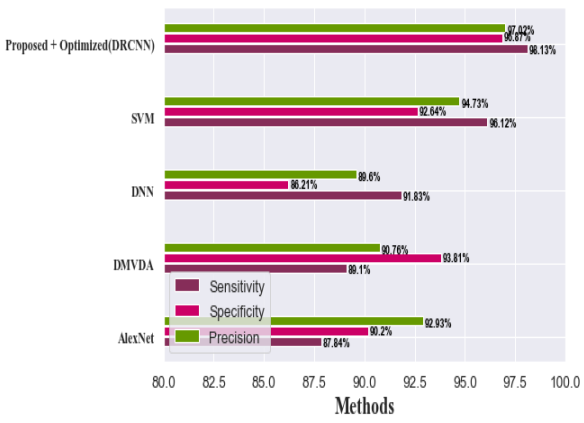

Figure 8. The proposed approach's categorization outcomes compared with existing approaches with optimization algorithm (a) Sensitivity, (b) Precision, and (c) Specificity.

An obtained higher Precision for the proposed approach is 97.02%, compared to 92.93% for AlexNet [19], 90.76% for DMVDA [20], 89.6% for DNN [21], and 94.73% for SVM [18]. Additionally, when compared to the previous approaches, the proposed method's specificity is higher. DNN [21] has the lowest accuracy rate, at 87.95 percent. The proposed approach categorization outcomes compared with the previous approaches with optimization algorithm graphs for specificity, precision, and sensitivity is demonstrated in Fig 9. Comparing with the previous approaches the proposed DRCNN approach obtained higher accuracy with the optimization algorithm. From the evaluation performance analysis, the performance of the categorization enhanced by utilizing the proposed approach, and computation time is decreased for training the pictures.

E. Evaluation of training results

Train Validation and Accuracy after 100 epochs, we obtained an accuracy of 97.54%, which is fairly impressive because accuracy curves eventually converge. The training and validation accuracy is displayed in Fig 9.

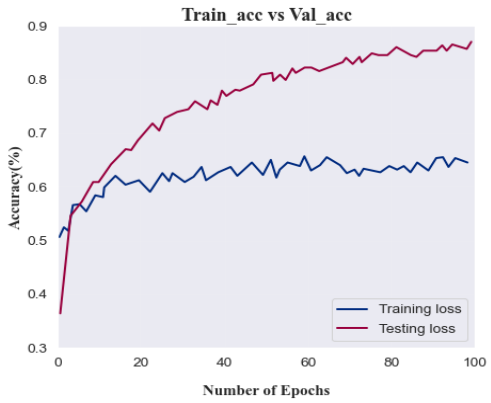

Figure 9. Training Vs Validation accuracy.

The validation Loss curve briefly fluctuates up and down. It proposes that more test results could be advantageous. However, because the variance between Test and Train Loss is minimal and the curve does not increase across epochs, this might be acceptable. The training and validation loss is displayed in Fig 10.

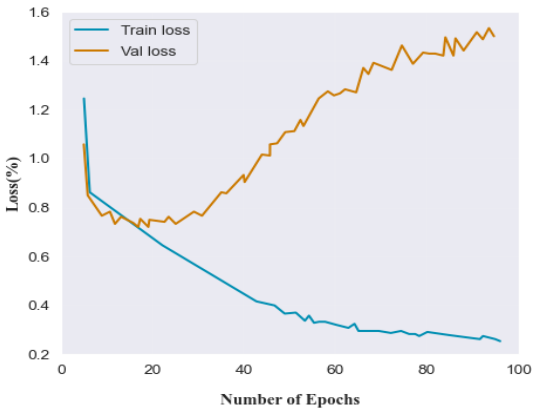

Figure 10. Training Vs Validation loss.

In Figs 9 and 10, the accuracy and loss during training are displayed. Better accuracy and loss estimates are being provided by the DRCNN. Our strategy outperforms previous approaches in the training and validation stages of the PD classification process.

F. Computation Time

Another aspect that is discussed is computation time. Deep learning techniques try to make computations less difficult. Comparing the computation times of our proposed DRCNN technique to those of other existing techniques is presented in Table 3. With minimal computing effort, it provides improved classification accuracy. Fig 11 shows how long it takes to compute utilizing the PPMI dataset using the most recent methodologies and the proposed model.

Approaches	**Computation Time (ms)**
AlexNet [19]	0.17
DMVDA [20]	0.21
DNN [21]	0.25
SVM [18]	0.24
Proposed (DRCNN)	0.15

Table 3 Utilizing the proposed and previous methods with optimization.

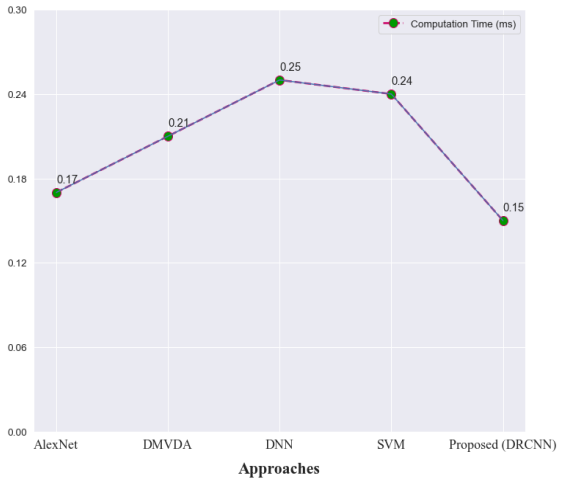

Figure 11. The time complexity of the proposed technique compared with the previous techniques

From Fig 11, it can be demonstrated that the proposed method exceeded computational time more than other techniques.

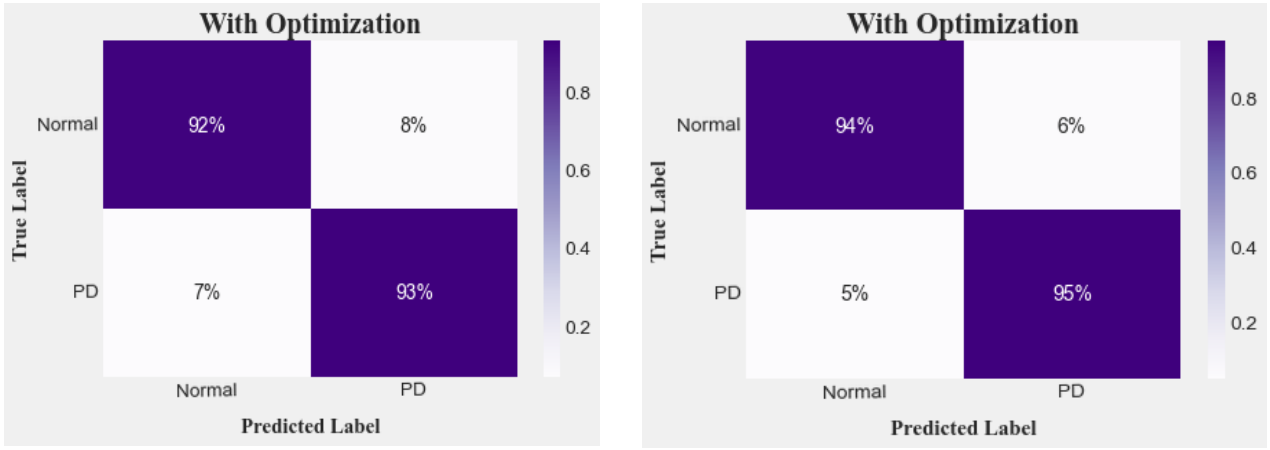

(a) (b)

Figure 12. Confusion matrix of PD (a) without optimization, and (b) with optimization

The most used technique for assessing categorization errors is the confusion matrix. The diagram shows that the DRCNN model can classify Parkinson's disease and Normal Health Control appropriately, with the PPMI dataset having the highest ratio of Parkinson's images and the lowest ratio of normal health control images. This shows that the proper categorization of the two statuses has been carried out. The obtained confusion matrix for the cross-validation test of classification is shown in Fig 12.

V. Conclusion

Parkinson's disease begins with very modest and perhaps undetectable primary causes, but the disease signs worsen. PD symptoms differ from person to person. In this paper, we proposed a technique to classify Parkinson's disease by MRI brain images. It has 4 steps to follow. Initially, normalize the input data using the min-max normalization method and then remove noise from input pictures utilizing a median filter. Then utilizing the Binary Dragonfly Algorithm to select the features. Furthermore, to segment the diseased part from MRI brain images using the technique Dense-UNet. Then, classify the disease as if it's Parkinson's disease or health control using the DRCNN technique along with Enhanced Whale Optimization Algorithm to get better classification accuracy. For these experimental results, we used Parkinson's MRI image-based Parkinson's Progression Marker Initiative (PPMI) dataset. This experiment gives 98.87% classification accuracy using the optimization algorithm. Our goal is to improve the deep learning model to several levels in future research to diagnose Parkinson's disease much more accurately.

Acknowledgements

We declare that this manuscript is original, has not been published before and is not currently being considered for publication elsewhere.

Reference

[1] O. O. Abayomi-Alli, R. Damaševičius, R. Maskeliūnas and A. Abayomi-Alli, "BiLSTM with data augmentation using interpolation methods to improve early detection of parkinson disease," *In 2020 15th Conference on Computer Science and Information Systems*, pp. 371-380, no.1, 2020.

[2] O. Yaman, F. Ertam, and T. Tuncer, "Automated Parkinson's disease recognition based on statistical pooling method using acoustic features", *Medical Hypotheses*, vol. 135, pp. 109483, 2020.

[3] A. Pasha, and P. H. Latha, "Bio-inspired dimensionality reduction for Parkinson's disease (PD) classification," *Health information science and systems*, vol. 8, no. 1, pp. 1-22, 2020.

[4] R. Lamba, T. Gulati, H. F. Alharbi and A. Jain, "A hybrid system for Parkinson's disease diagnosis using machine learning techniques," *International Journal of Speech Technology*, vol. 25, no. 3, pp. 583-593, 2022.

[5] E. Kaplan, E. Altunisik, Y. E. Firat, P. D. Barua, S. Dogan, M. Baygin and U. R. Acharya, "Novel nested patch-based feature extraction model for automated Parkinson's Disease symptom classification using MRI images," *Computer Methods and Programs in Biomedicine*, vol. 224, pp. 107030, 2022.

[6] Z. K. Senturk, "Early diagnosis of Parkinson's disease using machine learning algorithms," *Medical hypotheses*, vol. 138, pp. 109603, 2020.

[7] Z. Shu, P. Pang, X. Wu, S. Cui, Y. Xu and M. Zhang, "An integrative nomogram for identifying early-stage Parkinson's disease using non-motor symptoms and white matter-based radiomics biomarkers from whole-brain MRI," *Frontiers in aging neuroscience*, vol. 12, pp. 457, 2020.

[8] A. Mozhdehfarahbakhsh, S. Chitsazian, P. Chakrabarti, T. Chakrabarti, B. Kateb and M. Nami, "An MRI-based deep learning model to predict Parkinson's disease stages," *medRxiv*, 2021.

[9] L. Griffanti, J. C. Klein, K. Szewczyk-Krolikowski, R. A. Menke, M. Rolinski, T. R. Barber and C. Mackay, "Cohort profile: the Oxford Parkinson's Disease Centre Discovery Cohort MRI substudy (OPDC-MRI)", *BMJ open*, vol. 10, no. 8, pp. 34110, 2020.

[10] Y. Chen, G. Zhu, D. Liu, Y. Liu, T. Yuan, X. Zhang and J. Zhang, "The morphology of thalamic subnuclei in Parkinson's disease and the effects of machine learning on disease diagnosis and clinical evaluation," *Journal of the neurological sciences*, vol. 411, pp.116721, 2020.

[11] J. Luo, and J. F. Collingwood, "Effective R2 relaxation rate, derived from dual-contrast fast-spin-echo MRI, enables detection of hemisphere differences in iron level and dopamine function in Parkinson's disease and healthy individuals," *Journal of Neuroscience Methods*, vol. 382, pp. 109708, 2022.

[12] G. Prema Arokia Mary, N. Suganthi and M. S. Hema, "Early Prediction of Parkinson's disease from Brain MRI Images Using Convolutional Neural Network," *Journal of Medical Imaging and Health Informatics*, vol. 11, no. 12, pp. 3103-3109.

[13] M.R. Hossein-Tehrani, T. Ghaedian, E. Hooshmandi, L. Kalhor, A. A. Foroughi and V. R. Ostovan, "Brain TRODAT-SPECT Versus MRI Morphometry in Distinguishing Early Mild Parkinson's Disease from Other Extrapyramidal Syndromes," *Journal of Neuroimaging*, vol. 30, no. 5, pp. 683-689, 2020.

[14] T. Fu, M. Klietz, P. Nösel, F. Wegner, C. Schrader, G. U. Höglinger and X. Q. Ding, "Brain Morphological Alterations Are Detected in Early-Stage Parkinson's Disease with MRI Morphometry," *Journal of Neuroimaging*, vol. 30, no. 6, pp. 786-792, 2020.

[15] E. Porter, A. A. Roussakis, N. P. Lao-Kaim and P. Piccini, "Multimodal dopamine transporter (DAT) imaging and magnetic resonance imaging (MRI) to characterise early Parkinson's disease," *Parkinsonism & Related Disorders*, vol. 79, pp. 26-33, 2020.

[16] J. Zhang, Y. Li, Y. Gao, J. Hu, B. Huang, S. Rong and K. Nie, "An SBM-based machine learning model for identifying mild cognitive impairment in patients with Parkinson's disease," *Journal of the Neurological Sciences*, vol. 418, pp. 117077, 2020.

[17] G. Solana-Lavalle and R. Rosas-Romero, "Classification of PPMI MRI scans with voxel-based morphometry and machine learning to assist in the diagnosis of Parkinson's disease," *Computer Methods and Programs in Biomedicine*, vol. 198, pp.105793, 2021.

[18] E. Balaji, D. Brindha and R. Balakrishnan, "Supervised machine learning based gait classification system for early detection and stage classification of Parkinson's disease," *Applied Soft Computing*, vol. 94, pp. 106494, 2020.

[19] S. Sivaranjini and C. M. Sujatha, "Deep learning based diagnosis of Parkinson's disease using convolutional neural network," *Multimedia tools and applications*, vol. 79, no. 21, pp. 15467-15479.

[20] G. Nagasubramanian and M. Sankayya, "Multi-variate vocal data analysis for detection of Parkinson disease using deep learning," *Neural Computing and Applications*, vol. 33, no. 10, pp. 4849-4864.

[21] A. Caliskan, H. Badem, A. Basturk and M. Yuksel, "Diagnosis of the parkinson disease by using deep neural network classifier," *IU-Journal of Electrical & Electronics Engineering*, vol. 17, no. 2, pp. 3311-3318, 2021.

[22] M. Mafarja, I. Aljarah, A. A. Heidari, H. Faris, P. Fournier-Viger, X. Li, and S. Mirjalili, "Binary dragonfly optimization for feature selection using time-varying transfer functions," *Knowledge-Based Systems*, vol. 161, pp.185-204, 2018.

[23] J. Xin, X. Zhang, Z. Zhang and W. Fang, "Road extraction of high-resolution remote sensing images derived from DenseUNet," *Remote Sensing*, vol. 11, no. 21, pp. 2499, 2019.

[24] Z. Feng, A. Cai, Y. Wang, L. Li, L. Tong and B. Yan, "Dual residual convolutional neural network (DRCNN) for low-dose CT imaging," *Journal of X-Ray Science and Technology*, vol. 29, no. 1, pp. 91-109, 2021.

[25] S. Chakraborty, A. K. Saha, S. Sharma, S. Mirjalili and R. Chakraborty, "A novel enhanced whale optimization algorithm for global optimization," *Computers & Industrial Engineering*, vol. 153, pp. 107086, 2021.

Author Biographies

Praneeth Puppala is a student in the field of Computer Science and Engineering at Velagapudi Ramakrishna Siddhartha Engineering College. He is interested in the areas of Artificial intelligence, Machine learning and Data Science etc. Recently, he got placed in Tata Consultancy Services as a System Engineer.

Majety Sathvika is a student studying in Computer Science and Engineering at Velagapudi Ramakrishna Siddhartha Engineering College. She is interested in the areas of Artificial intelligence, Machine learning and deep learning. Recently, she got placed in AT&T as a Software Developer.

Vivek Kommareddy is a student in the field of Computer Science and Engineering at Velagapudi Ramakrishna Siddhartha Engineering College. He has a keen interest in the fields of bioinformatics, computer vision and artificial intelligence. Recently, he got placed in Deloitte.

Madala Sarath is a passionate student currently pursuing a bachelor's degree in Computer Science and Engineering at Velagapudi Ramakrishna Siddhartha Engineering College. With a keen interest in the dynamic fields of Artificial Intelligence, Machine Learning, and Data Science, Sarath is dedicated to expanding his knowledge and expertise in these domains. Recently, he got placed in Tata Consultancy Services as an Assistant System Engineer.

Saran Teja Mallela is an undergraduate student at Velagapudi Ramakrishna Engineering College pursuing a bachelor's degree in computer science and engineering. He worked on various initiatives involving machine learning in the medical field. He has a keen interest in the fields of dentistry, machine learning, and computer vision.

Dr. Koneru Suvarna Vani is currently working as a Professor in the Department of Computer Science and Engineering in Velagapudi Ramakrishna Siddhartha Engineering College, Andhra Pradesh. She received B.E (Computer Science and Engineering) Arulmigu Meenakshi Amman College of Engineering, Madras University, Madras in 1999, M.Tech (Computer Science and Engineering) Jawaharlal Nehru Technological University Anantapuram, Anantapuram in 2006 and Ph. D (Computer Science and Engineering) University of Hyderabad, Hyderabad in 2014, Her research interests are Bioinformatics and Machine Learning GIS.

Dr Prasun Chakrabarti has received his PhD degree in Computer Science and Engineering from Jadavpur University in 2009 and higher doctoral degree DLitt from Sambalpur University in 2022. In 2022 he has registered for another higher doctoral degree (DSc). He is working as Deputy Provost, ITM (SLS) Baroda University. He is Visiting Senior Scientist National Kaohsiung University of Science and Technology, Taiwan , Visiting Distinguished Research Fellow Wales Institute of Digital Information ,UK ; Honorary Adjunct Distinguished Professor Don State Technical University RUSSIA Visiting Professor Shiraz University of Medical Sciences IRAN, Honorary Visiting Distinguished Scientist PLANET Laboratory, Politecnico di Torino ITALY. His h index is 18 as per googl scholar.